Journal of General Virology (2016), **97**, 2769–2779 **DOI** 10.1099/jgv.0.000580

X-ray structure of *Triatoma virus* empty capsid: insights into the mechanism of uncoating and RNA release in dicistroviruses

Rubén Sánchez-Eugenia,[1] Aritz Durana,[1,2] Ibai López-Marijuan,[1,2] Gerardo A. Marti[3] and Diego M. A. Guérin[1,4]

Correspondence
Diego M. A. Guérin
diego.guerin@gmail.com

[1]Instituto Biofisika (CSIC, UPV/EHU), Barrio Sarriena S/N, 48940 Leioa, Bizkaia, Spain

[2]Fundación Biofísica Bizkaia, Barrio Sarriena S/N, 48940 Leioa, Bizkaia, Spain

[3]Centro de Estudios Parasitológicos y de Vectores (CEPAVE-CCT-La Plata-CONICET-UNLP), Boulevard 120 e/61 y 62, 1900 La Plata, Argentina

[4]Departamento de Bioquímica y Biología Molecular, Facultad de Ciencia y Tecnología, Universidad del País Vasco (UPV/EHU), Barrio Sarriena S/N, 48940 Leioa, Bizkaia, Spain

In viruses, uncoating and RNA release are two key steps of successfully infecting a target cell. During these steps, the capsid must undergo the necessary conformational changes to allow RNA egress. Despite their importance, these processes are poorly understood in the family *Dicistroviridae*. Here, we used X-ray crystallography to solve the atomic structure of a *Triatoma virus*(TrV) empty particle (Protein Data Bank ID 5L7O), which is the resulting capsid after RNA release. It is observed that the overall shape of the capsid and of the three individual proteins is maintained in comparison with the mature virion. Furthermore, no channels indicative of RNA release are formed in the TrV empty particle. However, the most prominent change in the empty particle when compared with the mature virion is the loss of order in the N-terminal domain of the VP2 protein. In mature virions, the VP2 N-terminal domain of one pentamer is swapped with its twofold related copy in an adjacent pentamer, thereby stabilizing the binding between the pentamers. The loss of these interactions allows us to propose that RNA release may take place through transient flipping-out of pentameric subunits. The lower number of stabilizing interactions between the pentamers and the lack of formation of new holes support this model. This model differs from the currently accepted model for rhinoviruses and enteroviruses, in which genome externalization occurs by extrusion of the RNA through capsid channels.

Received 8 July 2016
Accepted 12 August 2016

INTRODUCTION

Triatoma virus (TrV) is a positive-sense ssRNA virus that belongs to the family *Dicistroviridae* and genus *Cripavirus* within the order *Picornavirales*. The type species of this genus is *Cricket paralysis virus* (CrPV). TrV is a lethal pathogen for different insect species of the Triatominae subfamily (Hemiptera: Reduviidae), including *Triatoma infestans*, one of the main vectors for the transmission of the protozoon *Trypanosoma cruzi* (Marti *et al.*, 2013; Muscio *et al.*, 1988). This protozoon is the causative pathogen of Chagas disease (American trypanosomiasis), a neglected disease that is endemic in Latin America affecting about eight million people (Grayson *et al.*, 2010). Thus, TrV has been proposed as a biological control agent against the spread of Chagas disease (Bonning & Miller, 2010; Czibener *et al.*, 2000; Muscio *et al.*, 1997; Querido *et al.*, 2013).

Dicistroviridae and *Picornaviridae* are closely related families due to their similarities in genome organization, protein composition and capsid structure. Both families are so similar that dicistroviruses were initially referred to as picorna-like viruses (Muscio *et al.*, 1988). However, whereas the genome of picornaviruses has a single ORF, the genome of dicistroviruses is divided into two different ORFs that separately code for the structural and non-structural proteins. This difference was the main reason for the establishment of *Dicistroviridae* as a new family (Mayo, 2002). The first ORF codes for the non-structural proteins (helicase, protease and RNA-dependent RNA polymerase) and the second ORF codes for a unique protein called P1, which is the precursor of the four structural proteins that build the

Two supplementary figures are available in the online Supplementary Material.

capsid (from the N terminus to the C terminus: VP2, VP4, VP3 and VP1). Once the P1 precursor has been cleaved into VP2, VP0 (VP4+VP3) and VP1 by the coded viral protease, the particle assembles and VP0 undergoes autoproteolytic cleavage into its components in an RNA-dependent manner (Agirre *et al.*, 2011; Sánchez-Eugenia *et al.*, 2015b). The assembled particle consist of a pseudo *P*=3 icosahedral capsid that is 30 nm in diameter built by 60 copies of each structural protein with the VP1–VP3 proteins folded in a so-called *jelly roll* core [Protein Data Bank (PDB) code 3NAP; Squires *et al.*, 2013]. The salient structural features of TrV that differentiate it from enteroviruses and rhinoviruses are the lack of a large depression around the fivefold axes called the *canyon*, the absence of the hydrophobic pocket and the swapping of the VP2 N-terminal domain (Squires *et al.*, 2013). These important differences between the structures of these viruses suggest that the mechanisms involved in receptor binding, capsid stabilization, uncoating and RNA release may be different to those of enteroviruses and rhinoviruses. However, a recently solved structure of the picornavirus *Hepatovirus A* (Wang *et al.*, 2015) shows the characteristic VP2 domain swapping thought to be specific to dicistroviruses. This observation led the authors to propose that *Hepatovirus A* may be a phylogenetic link between dicistroviruses and picornaviruses, and it may uncoat through a novel mechanism.

In this work, we focus on the structural changes that the TrV capsid undergoes upon genome delivery, a key process in the infective cycle of all viruses. During this process, the capsid must undergo the necessary conformational changes to allow the RNA to egress. Through these steps, the cellular membranes must be breached; thus, both picornaviruses and dicistroviruses code small hydrophobic proteins, called VP4, which are involved in membrane permeation (Panjwani *et al.*, 2014; Sánchez-Eugenia *et al.*, 2015a). For picornaviruses the mechanisms for uncoating and RNA release are somewhat understood. Although picornaviruses share common structural features, they cluster into two groups regarding their uncoating mechanism. For enteroviruses and rhinoviruses from the genus *Enterovirus* of the family *Picornaviridae*, the first proposed model for uncoating and RNA release stated that RNA egressed through a widened fivefold axis (Belnap *et al.*, 2000; Bubeck *et al.*, 2005; Hewat & Blaas, 2004; Hewat *et al.*, 2002; Xing *et al.*, 2003). However, recent evidence supports a model in which upon receptor binding and pocket factor dislodgment, the capsid expands and externalizes the VP1 N terminus and VP4. These conformational changes lead to the release of the RNA through a small pore formed at the twofold axis (Bostina *et al.*, 2011; Garriga *et al.*, 2012; Levy *et al.*, 2010; Shingler *et al.*, 2013; Wang *et al.*, 2012). In support of this model, the structure of the resulting enterovirus and rhinovirus empty particles (B-particles or 80S particles; after RNA egress) and intermediate expanded particles (A-particles or 135S-particles; they still contain the RNA but are primed for its release) have been solved by cryo-electron microscopy (cryo-EM) and X-ray crystallography (Garriga *et al.*, 2012; Pickl-Herk *et al.*, 2013; Ren *et al.*, 2013; Shingler *et al.*, 2013). The crystallographic structure of the empty particle of human rhinovirus type 2 (HRV2) and enterovirus 71 (EV71) shows a capsid whose N-terminal regions of VP1 are disordered and whose protomers have been displaced, forcing the rearrangement of the interprotomer interfaces and resulting in the opening of channels at the base of the canyon and at the twofold axes (Garriga *et al.*, 2012; Shingler *et al.*, 2013). The channel at the base of the canyon was proposed to allow the externalization of the VP1 N terminus, and the channel at the twofold axis is thought to allow RNA release. Alternatively, the structure of the uncoating-intermediate particle (A-particle) of the three viruses HRV2, EV71 and coxsackievirus A16 shows that the N-terminal region of VP1 interacts with RNA near the twofold axis that is already opened (Pickl-Herk *et al.*, 2013; Ren *et al.*, 2013; Shingler *et al.*, 2013). These recent results support, as previously described, that RNA release in enteroviruses and rhinoviruses takes place through channels at the twofold axes via the externalization of VP1 N-terminal residues. In contrast, viruses from the genera *Aphthovirus* and *Cardiovirus* of the family *Picornaviridae* are thought to release their RNA by direct dissociation into pentamers at low pH (Baxt & Bacharach, 1980; Brown & Cartwright, 1961; Tuthill *et al.*, 2009). However, recent structural evidence shows that RNA release in aphthoviruses may also proceed via a transient empty capsid prior to the dissociation state similar to the mechanism used by enteroviruses and rhinoviruses (Tuthill *et al.*, 2009) or through a massively expanded particle with large pores (Bakker *et al.*, 2014). In any case, the details of the structural changes that allow RNA egress in aphthoviruses are less well understood than those of enteroviruses and rhinoviruses.

Unlike picornaviruses, knowledge of the process of uncoating and RNA release in dicistroviruses is still very poor. A low-resolution (22 Å) cryo-EM reconstruction of TrV empty particles obtained by heat treatment showed that upon RNA release, TrV did not display any prominent conformational changes with respect to full virions: the protein shell size and thickness were identical (Agirre *et al.*, 2013). Moreover, TrV is not acid-labile, which excludes low endosomal pH as the RNA release trigger (Agirre *et al.*, 2011; Snijder *et al.*, 2013). However, increased pH does destabilize the genome–capsid interactions triggering the disassembly of the capsid into pentameric subunits along with the release of the RNA and VP4 (Snijder *et al.*, 2013). Furthermore, as previously mentioned, the TrV capsid lacks the pocket factor, which has been shown to be required in the uncoating of enteroviruses and rhinoviruses from the related genus *Enterovirus* of the family *Picornaviridae* (Grant *et al.*, 1994; Smith *et al.*, 1986; 1995; Zhang *et al.*, 2008). Other picornaviruses however, also lack the pocket factor.

All of these data indicate that the uncoating process in dicistroviruses will presumably be different from that of picornaviruses. Since the low-resolution cryo-EM reconstructions did not provide structural insight into the changes occurring

during RNA release, we solved the structure of the TrV empty capsid at 3.6 Å resolution in this study (PDB code 5L7O). The aim of this work is to address the uncoating mechanism of this virus from the poorly studied family *Dicistroviridae*. Here, we show that after RNA release, the overall structure of the particle is maintained. The most prominent changes in the empty TrV capsid in comparison to the full particle are the narrowing of the fivefold axis cavity, the absence of new holes and the loss of the twofold domain swapping that stabilizes the binding between the pentameric subunits.

RESULTS AND DISCUSSION

Native TrV virions were emptied by heating full virions to 56 °C for 12 min. Heating has been used to create empty virions in other picornaviruses and also in previous TrV studies (Agirre *et al.*, 2011; Belnap *et al.*, 2000; Bostina *et al.*, 2011; Bubeck *et al.*, 2005; Garriga *et al.*, 2012; Hewat & Blaas, 2004; Hewat *et al.*, 2002; Levy *et al.*, 2010; Shingler *et al.*, 2013; Wang *et al.*, 2012; Xing *et al.*, 2003); this technique exploits the idea that the empty particles generated by heating are thought to be identical to those naturally emptied. The structure of these empty capsids (PDB code 5L7O) was solved at 3.6 Å resolution by molecular replacement using the structure of the native virion previously solved at 2.5 Å resolution (RCSB PDB code 3NAP; Squires *et al.*, 2013) as the starting model. After rebuilding, non-crystallographic symmetry (NCS)-constrained refinement and density averaging cycles, the final model represented the conformational changes that occurred in the capsid due to the release of RNA and VP4.

Analysis of structural changes

Individual viral proteins. The overall shapes of the three structural proteins VP1, VP2 and VP3 are maintained in the empty capsid compared to the native virion (Fig. 1).

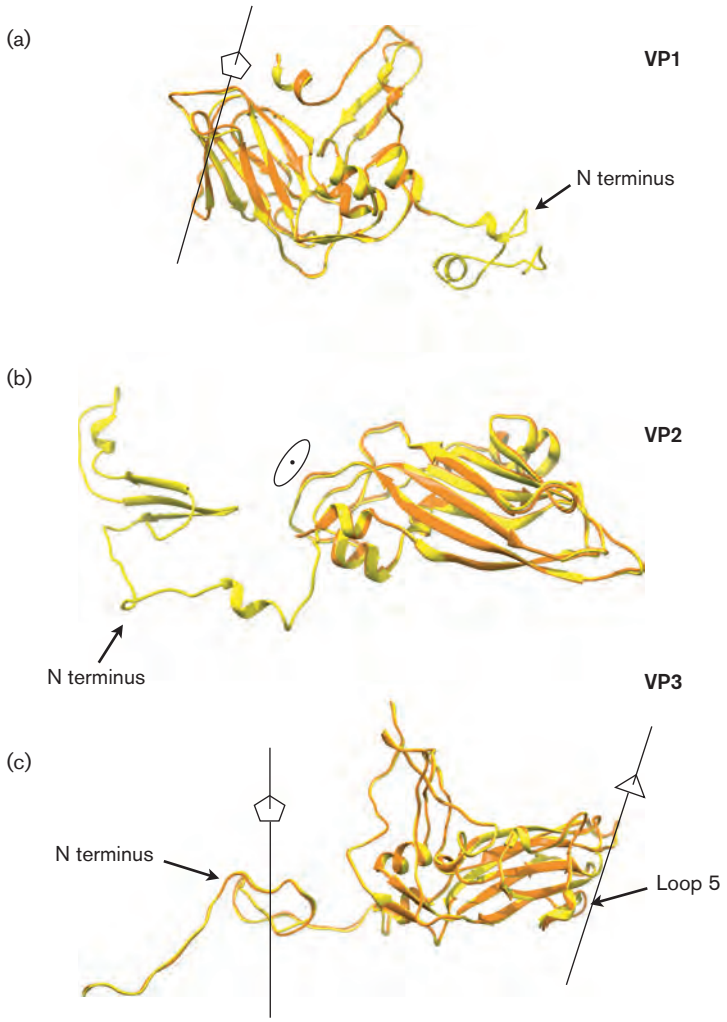

Fig. 1. Superimposition of individual viral proteins of native and empty TrV. The β-barrel of VP1 (a), VP2 (b) and VP3 (c) proteins between the full virion (yellow) and the empty particle (orange) are superimposed. The structural motifs showing the biggest differences are indicated.

The most prominent change was the lack of density for the first 33 N-terminal residues of VP1 and for the first 76 N-terminal residues of VP2 (Fig. S1, available in the online Supplementary Material). These residues, which were ordered from position 1007 in VP1 and 2009 in VP2 in the mature virion, were disordered in the empty capsid (note that the residues of VP1, VP2 and VP3 are numbered using 1000, 2000 and 3000, respectively). This lack of order was also observed in the N terminus of VP1 protein in the empty capsid of HRV2 (Garriga *et al.*, 2012). In a low-resolution (22 Å) cryo-EM reconstruction of empty TrV capsids (Agirre *et al.*, 2013), an extra density located at the exterior of the twofold symmetry axes was modelled as a rigid movement of the N terminus of VP2 toward the capsid exterior. However, in the present crystallographic study, no density was present to build a structural model of any of the N-terminal VP2 residues in the capsid interior, across the shell or at the capsid exterior. We hypothesize that these disordered regions, which in the mature virion are ordered inside the capsid, may interact with the RNA or may interact with other parts of the inner capsid favoured by the presence of the RNA. In either case, these interactions may contribute to the stability of the full virion. However, in the previously solved structure of the native virion (Squires *et al.*, 2013) the RNA was not visible and thus, these points cannot be proven. Since RNA has been released in the empty capsid, these interactions would be lost, which could lead to the observed disorder in these regions.

Superimposition between the viral proteins from the empty capsid and from the mature virion (shown in Fig. 1) was performed for each VP by aligning the jelly roll β-barrel. These regions were very similar between both models with an root-mean-square deviation (RMSD) for the Cα atoms of the jelly roll of 0.25, 0.34 and 0.32 Å for VP1, VP2 and VP3, respectively (in the following, RMSD values refer to the same comparison). The most noticeable changes were concentrated in the N- and C-terminal regions as well as in some of the loops between the β sheets.

As previously mentioned, VP1 lacked electron density for in the first 33 N-terminal residues. In the mature virion, these 33 amino acids are in close contact and establish stabilizing ionic interactions with the VP2 N-terminal region of an adjacent protomer of the same pentamer (see Fig. 4). However, in the empty capsid, both N-terminal regions are disordered, and these interactions are lost. Furthermore, the lack of order in one N-terminal region probably leads to disorder in the other. The region comprising amino acid residues 1191–1195 seems especially flexible, since the average B factor of this region (195 Å^2) is markedly higher than that of VP1–VP3 (Table 1).

In VP2, the disordered region corresponds to the first 76 amino acids, which is 30 % of the protein. These missing residues are key in the assembly of the native particles because they exchange with their twofold related counterparts in the neighbouring pentamer, thereby stabilizing the interpentameric complexes and, thus, the capsid by domain swapping (Fig. 4, Table 2; Bennet *et al.*, 1995; Squires *et al.*, 2013). In the empty capsid, all of these interactions are lost. The region between the first observed amino acid (Thr2077) and the first residue of the first β sheet of the jelly roll (Gln2088) has the highest RMSD in VP2 (0.99 Å). This is basically because amino acids 2077–2079, the first three observed amino acids, are shifted at approximately 2 Å.

Regarding the VP3 protein, no amino acids become disordered upon RNA release. Loop 5 (aa 3170–3175) with an RMSD of 1.57 Å is the loop with the largest shift. This change is essentially centred on amino acids 3171–3173 and corresponds to a 3 Å shift of these residues toward the β sheets of VP3. This displacement leads to the rearrangement of the interactions with VP2 protein of a neighbouring pentamer (Table 4). The N-terminal region of VP3 (aa 3001–3064), which partially forms the inner region of the fivefold cavity, also deviates to some extent from the native model.

Pentameric structure. The small displacements in the amino acids of VP1, VP2 and VP3 give rise to a pentamer

Table 1. Data collection and refinement statistics

CC1/2 stands for the Pearson correlation coefficient between two random halfs of unique reflections. CC* stands for the estimation of the real correlation coefficient between the averaged data-set and the noise-free t signal.

TrV empty capsid	
Data collection	
Wavelength (Å)	0.9795
Resolution range	47.7–3.6 (3.7– 3.6)
Space group	R3 : H
Unit cell	305.59 Å, 305.59 Å, 796.49 Å; 90 °, 90 °, 120 °
Total reflections	684 874 (67 652)
Multiplicity	2.2 (2.2)
Completeness	0.98 (0.97)
R-merge	0.162 (1.32)
CC1/2	0.985 (0.196)
CC*	0.996 (0.573)
Refinement	
Resolution range (Å)	47.7–3.6
Reflection used for Rfree	6427
Rwork	0.268
Rfree	0.269
RMSD bonds (Å)	0.007
RMSD angles (°)	1.19
Ramachandran favoured (%)	91
Ramachandran allowed (%)	8.5
Ramachandran outliers (%)	0.15
Average B-factor (Å^2)	114.3

Table 2. Summary of protein–protein interactions in mature TrV and in the empty capsid

M–M, Interactions between main chains; M–S, interactions between main and side chains; S–S, interactions between side chains.

		Ionic	H-bonds			Aromatic	
			M–M	M–S	S–S	π–π	π–Cation
Intrapentamer	Mature	20	56	155	116	12	6
	Empty	12	30	139	43	10	5
Interpentamer	Mature	14	20	138	14	10	10
	Empty	3	1	49	30	5	5

that mostly maintains its structure compared to the native virion and that only has an appreciable change in the fivefold cavity. This cavity is essentially formed (from the capsid outside to inside) by rings of Gln1128, Val1166, Thr1167, Gln3014 and Val3012. The minimal changes in the positions of these residues maintain the overall cavity diameter except for Gln3014, which seems to shift toward the lumen of the cavity, narrowing the diameter of the region at that position (Fig. 2) (note that the error in the atomic coordinates of this structure at 3.6 Å resolution can lead to ambiguous interpretations of these displacements). In this way, the fivefold cavity appears to preclude the transit of ions between the capsid inside and outside as shown by the solvent accessible surface (Fig. 2). In enteroviruses and rhinoviruses from the related family *Picornaviridae*, the apparent enlargement of the fivefold cavity in empty capsids, shown initially by cryo-EM, was used to propose a model in which RNA exited the capsid through this widened channel (Belnap *et al.*, 2000; Bubeck *et al.*, 2005; Hewat & Blaas, 2004; Hewat *et al.*, 2002; Rossmann *et al.*, 2002; Xing *et al.*, 2003). However, current crystallographic data in enteroviruses and rhinoviruses (Garriga *et al.*, 2012; Wang *et al.*, 2012) shows that the fivefold cavity is constricted. This, which is also observed here for TrV, makes RNA release through this cavity unlikely. Nevertheless the time- and space-averaged crystallographic data cannot exclude the occurrence of large transient conformational changes leading to the opening of the cavity.

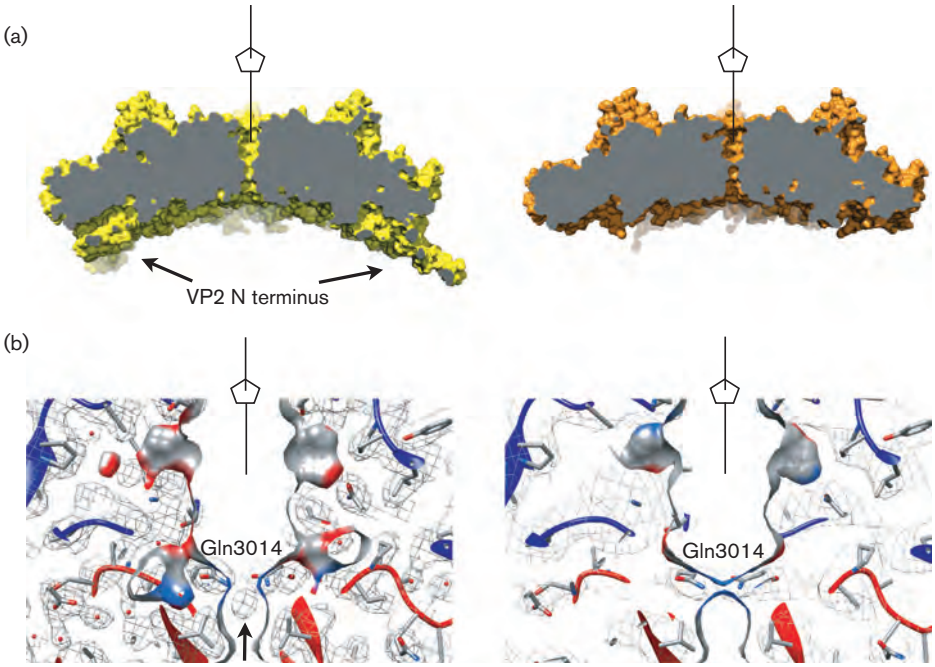

Fig. 2. Narrowing of the fivefold cavity. (a) The solvent accessible surface of the pentameric subunit is clipped to show the fivefold channel in yellow (left) for the mature virion and in orange (right) for the empty particle. It can be observed that the empty particle channel is closed while that of the mature virion is not. (b) Electron density populating the fivefold channel of the mature virion (left) and the empty capsid (right). For clarity, the atomic model, the electron density and the surface representation are clipped. In the central region of the channel of the mature virion, different Gln3014 residues coordinate a density, which likely corresponds to a cation. However, in the empty capsid, this density is lost and the channel is collapsed.

Additionally, in the structures of both mature TrV (Squires *et al.*, 2013) and mature CrPV (Tate *et al.*, 1999), a spherical density was found at the fivefold cavity. This density was interpreted as a metal cation that in TrV was coordinated to the oxygen atom of the side chain of Gln3014 (Squires *et al.*, 2013). In the empty capsid structure, no density is observed at the same position (Fig. 2b), indicating that the putative cation found in native TrV was released as a consequence of RNA egress. As the presence of cations in the fivefold axes of some viruses in the order *Picornavirales* has been shown to be relevant in the stabilization of their structure (Zhao *et al.*, 1997), the loss of this cation may be related to the destabilization of the capsid to allow TrV uncoating.

Furthermore, no pores are formed near the canyon in the pentameric subunits of the empty capsid of TrV, which is a major difference compared with the HRV2 empty particle (Garriga *et al.*, 2012). In our case, the surface of the pentamer in the empty capsid of TrV is almost identical to that of the mature virion. In HRV2, the observed pores were interpreted as the remainder of the VP1 N-terminal externalization, but there is no evidence of VP2 N-terminal region externalization in our case.

Overall capsid structure. The overall capsid structure and icosahedral symmetry of the empty particle is conserved in comparison to the mature virion. The outer diameter of the capsid is roughly the same (33 nm) in both particles (Fig. 3), and the only difference in thickness is mainly due to the missing N-terminal regions of VP2 that would lie below the twofold axes. This similarity between the empty and full particles in TrV contrasts the pronounced changes found between these particles in enteroviruses and rhinoviruses. The protomer rearrangement in the empty capsids of both rhinovirus (Garriga *et al.*, 2012) and enterovirus (Wang *et al.*, 2012) led to a particle expansion of approximately 4 % in diameter and a protein shell thinning of approximately 10 %. However, in the TrV empty particles, the alterations in the positions of the proteins are not prominent enough to induce those overall conformational changes in the capsid.

Interaction rearrangement and RNA release model

Rearrangement of intrapentameric interactions. In the previous section, we described all of the conformational changes that occurred in the TrV capsid upon RNA release. These changes, along with the disorder of the N-terminal domains, lead to the loss of several amino acid interactions and to the formation of new interactions. In the native virion, each protomer establishes a total of 365 interactions that are predicted to be attractive (Table 2) and to stabilize the pentamer: 20 ionic interactions, 327 hydrogen bonds and 18 aromatic interactions. In the empty capsid, the interaction network is weaker with only 239 interactions being conserved: 12 ionic interactions, 212 hydrogen bonds and 15 aromatic interactions.

Focusing on the ionic contacts, of the 20 present in mature virions, 12 are lost and four new interactions are formed (Table 3). VP1 loses five interactions: three of them are located in the disordered N-terminal portion (aa 1009, 1017 and 1019) that interacts with an adjacent VP2. The other two (Glu1041 and Glu1172, which is near the fivefold axis) no longer interact with different VP3 proteins. On the other hand, VP1 establishes two new ionic contacts near the spikes: Asp1142 and Arg1243 interact with two different VP1 proteins. In the case of VP2, five interactions are lost as a consequence of the disorder of its N-terminal region: the three interactions missing with an adjacent VP1 previously described and two other interactions lost between the N-terminal residues of other intrapentameric VP2 proteins. VP2 does not establish any new interactions. Finally, as previously described, VP3 loses two interactions with VP1 and establishes two new interactions: Lys3002 and Asp3027 interact with two different VP3 proteins (Table 3).

All these missing intrapentameric interactions, which are mainly focused on the VP1 and VP2 N-terminal domains, apparently do not strongly affect the structural integrity of the pentamers. Thus, it can be suggested that the empty capsid pentamers are still robust building blocks for the maintenance of the viral capsid. This result coincides with previous results showing that upon alkaline-dependent uncoating, the disassembly intermediates of TrV were pentameric subunits (Snijder *et al.*, 2013).

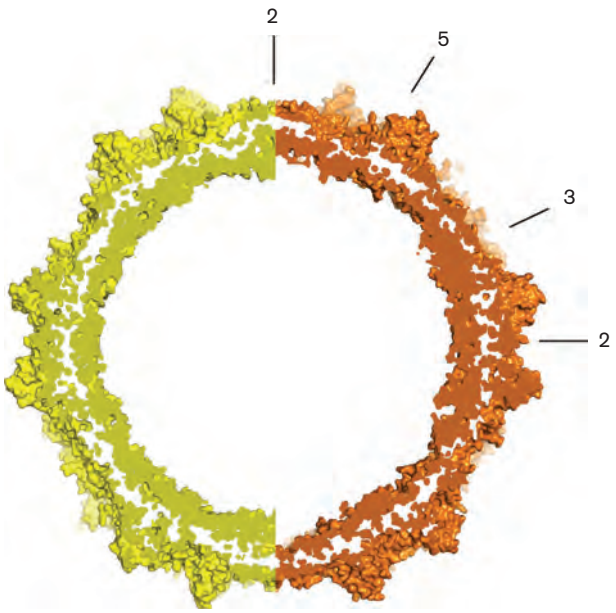

Fig. 3. Overall capsid structure comparison. The solvent-accessible surface of the native viral particle (yellow) and of the empty particle (orange) is shown. The particles are oriented in the same way and are clipped to show only their central section. Only half of each capsid is shown for comparison.

Rearrangement of interpentameric interactions. In the TrV empty capsid, the rearrangement of the interactions between protomers of different pentamers is more extensive than the rearrangement within pentamers. In the native virion, each protomer establishes a total of 206 interactions (Table 2) that are predicted to stabilize the binding between adjacent pentamers: 14 ionic interactions, 172 hydrogen bonds and 20 aromatic interactions. In the empty capsid, the positional changes caused by RNA release lead to a weakened interaction network where only 93 interactions are conserved: 3 ionic interactions, 80 hydrogen bonds and 10 aromatic interactions.

As in the intrapentameric case, we will focus our analysis on the ionic contacts. From the 14 ionic interactions present in mature virions, two new interactions are created and 13 are lost (Table 4). Twelve of these 13 interactions are lost as a consequence of the disordered VP2 N-terminal regions (Fig. 4): two are lost with its twofold related counterpart (His2049–Glu2190), four with other VP2s (Asp2018–Arg2024 and Lys2028–Glu2056), four with an adjacent VP1 (Arg2070–Glu1033 and Arg2070–Asp1035) and two with an adjacent VP3 (Asp2068–Lys3043). The last missing interaction, which is not a consequence of the disordered VP2 N-terminal residues, is between Glu2121 and Arg3159 of an adjacent VP3. This interaction is also located at the twofold axis.

As illustrated in the previous paragraphs, the N-terminal domain of VP2 is a key region in stabilizing the binding between the pentameric subunits to build the full capsid of the mature virions in dicistroviruses. However, in TrV empty capsid ~80 % of these interactions are lost as a result of the disorder of the first 76 residues of VP2 (Fig. 4). As the reduction in the number of interactions can be interpreted as a weaker overall interaction, we conclude that this rearrangement of interactions produces a capsid whose pentamers are weakly bound at the twofold symmetry axes due to the loss of the domain swapping.

Model for RNA release. Taking into account that the empty capsid structure is the final snapshot of the RNA release process, the structural changes and the weakening of the interpentameric interfaces allow us to discuss possible

Table 3. Intrapentameric ionic interactions

Chain organization is as follows: the reference protomer is numbered as 1 and the other four protomers are numbered 2, 3, 4 and 5 clockwise as shown in Fig. S2.

Interaction						Mature TrV	Empty capsid
Residue 1			Residue 2				
Amino acid no.	Residue	Chain	Amino acid no.	Residue	Chain		
1009	Arg	1VP1	2022	Glu	2VP2	Yes	No
1017	Glu	1VP1	2028	Lys	2VP2	Yes	No
1019	Lys	1VP1	2027	Glu	5VP2	Yes	No
1041	Glu	1VP1	3043	Lys	2VP3	Yes	No
1052	Glu	1VP1	3035	Lys	2VP3	Yes	Yes
1142	Asp	1VP1	1243	Arg	5VP1	No	Yes
1142	Asp	1VP1	3200	Arg	5VP3	Yes	Yes
1151	Asp	1VP1	1243	Arg	5VP1	Yes	Yes
1163	Glu	1VP1	3015	Arg	5VP3	Yes	Yes
1172	Glu	1VP1	3015	Arg	5VP3	Yes	No
1243	Arg	1VP1	1142	Asp	2VP1	No	Yes
1243	Arg	1VP1	1151	Asp	2VP1	Yes	Yes
2022	Glu	1VP2	1009	Arg	5VP1	Yes	No
2027	Glu	1VP2	1019	Lys	5VP1	Yes	No
2028	Lys	1VP2	1017	Glu	5VP1	Yes	No
2033	Glu	1VP2	2187	Lys	5VP2	Yes	No
2187	Lys	1VP2	2033	Glu	2VP2	Yes	No
3002	Lys	1VP3	3027	Asp	4VP3	No	Yes
3015	Arg	1VP3	1163	Glu	2VP1	Yes	Yes
3015	Arg	1VP3	1172	Glu	2VP1	Yes	No
3027	Asp	1VP3	3002	Lys	2VP3	No	Yes
3035	Lys	1VP3	1052	Glu	5VP1	Yes	Yes
3043	Lys	1VP3	1041	Glu	5VP1	Yes	No
3200	Arg	1VP3	1142	Asp	2VP1	Yes	Yes

Table 4. Interpentameric ionic interactions

Chain organization is as follows: the reference pentamer is called 'a' , and the three surrounding pentamers are called 'b', 'c' and 'd' as shown in Fig. S2.

Interaction						Mature TrV	Empty capsid
Residue 1			Residue 2				
Amino acid no.	Residue	Chain	Amino acid no.	Residue	Chain		
1033	Glu	aVP1	2070	Arg	dVP2	Yes	No
1035	Asp	aVP1	2070	Arg	dVP2	Yes	No
2018	Asp	aVP2	2024	Arg	cVP2	Yes	No
2024	Arg	aVP2	2018	Asp	bVP2	Yes	No
2028	Lys	aVP2	2056	Glu	bVP2	Yes	No
2049	His	aVP2	2190	Glu	bVP2	Yes	No
2056	Glu	aVP2	2028	Lys	cVP2	Yes	No
2068	Asp	aVP2	3043	Lys	cVP3	Yes	No
2070	Arg	aVP2	1033	Glu	cVP1	Yes	No
2070	Arg	aVP2	1035	Asp	cVP1	Yes	No
2121	Glu	aVP2	3159	Arg	cVP3	Yes	No
2190	Glu	aVP2	3136	Arg	cVP3	No	Yes
2190	Glu	aVP2	2049	His	cVP2	Yes	No
3043	Lys	aVP3	2068	Asp	cVP2	Yes	No
3136	Arg	aVP3	2190	Glu	dVP2	No	Yes
3159	Arg	aVP3	2121	Glu	dVP2	Yes	Yes

RNA release models for TrV. Importantly, the constriction of the fivefold cavity makes RNA release through this region very unlikely. Moreover, the absence of pores, channels or any other sign of RNA crossing through the capsid, features observed in enteroviruses and rhinoviruses (Bostina *et al.*, 2011; Garriga *et al.*, 2012; Wang *et al.*, 2012), points to an uncoating mechanism different to that of these picornaviruses. The results presented here can be congruent with different RNA release models: (i) the virion capsid may totally or partially disassemble into pentameric subunits, thus releasing RNA; then these pentamers would reassemble into an empty capsid. (ii) The empty capsid solved here may be the resulting particle subsequent to a swollen particle with large holes that would allow RNA egress. This expanded particle has been found and its structure has been solved by cryo-EM, in aphthoviruses (Bakker *et al.*, 2014),

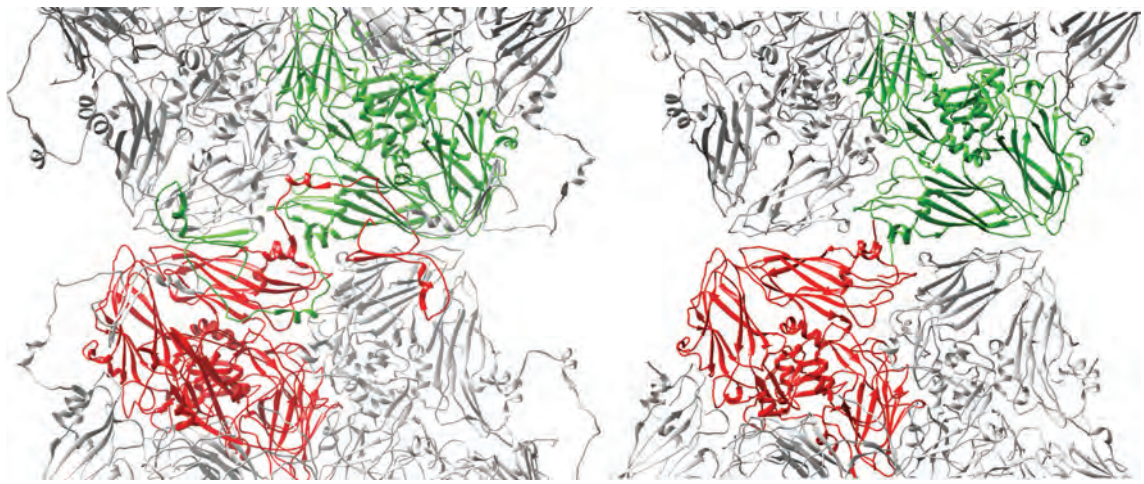

Fig. 4. Domain swapping at the twofold axis. The interface between two pentamers is shown at the twofold axis for the interior of the full virion (left) and for the interior of the empty capsid (right). Two protomers are highlighted in green and red, one from each pentamer. In the full virion, domain swapping is clearly visible as an exchange between identical domains of both highlighted protomers. However, this largely stabilizing feature is absent in the empty capsid.

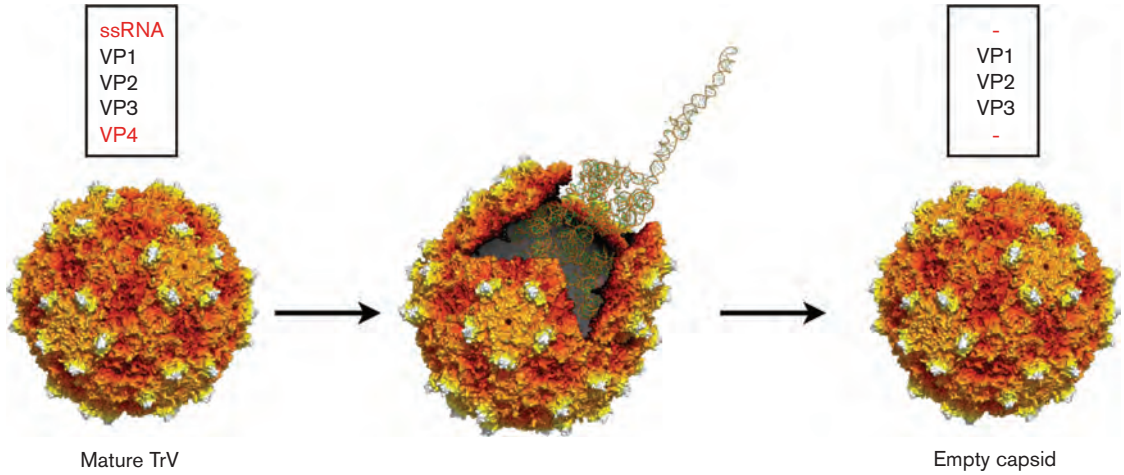

Fig. 5. One of the possible models for the uncoating and RNA release processes in TrV. After triggering the uncoating mechanism, the pentameric subunits of the mature virion may flip out over their twofold axis forming transient openings in the capsid. Once RNA has been released, these pentameric subunits would flip back again to form the empty capsid.

but this putative uncoating intermediate seems to lack the capacity to turn into a not-expanded empty particle. And finally, (iii) pentameric subunits may flip out over their destabilized interface at the twofold axis remaining attached via other interface. Then, after RNA release, they would flip back again to form the empty capsid (Fig. 5).

Even though all of these models are feasible with the results shown here, we hypothesize that the third model is the most likely. This model (Fig. 5), in which pentameric subunits may flip out and flip back again, would result in the transient formation of openings in the capsid due to the weakened interpentameric interfaces. These transient openings would allow RNA translocation. The weakening of the binding between pentamers and the nearly unchanged structure of the pentamer support this model, which may hold for other members of the family *Dicistroviridae*. Nevertheless, at this point the exact mechanism used by TrV to uncoat and translocate its RNA into the target cell cannot be definitely stated.

METHODS

Materials. Pentaerythritol propoxylate 629, Tris-HCl and magnesium chloride were purchased from Jena Bioscience. Sucrose and sodium chloride were purchased from Sigma-Aldrich.

Generation and crystallization of empty particles. Mature TrV virions were purified from experimentally infected *Triatoma infestans* faeces by centrifugation as previously described (Agirre *et al.*, 2011). Full particles at 0.05 mg ml^{-1} in 50 mM Tris pH 7, 10 mM NaCl, 1 mM $MgCl_2$, were emptied by incubation at 56 °C for 12 min with continuous shaking. After assessing the emptying yield by negative-staining transmission electron microscopy, the solution was concentrated to 3 mg ml^{-1} using Amicon Centrifuge Filters (Millipore). Crystals were grown at 18 °C by vapour diffusion in sitting drop plates by mixing equal volumes of the capsid solution and the reservoir solution: 100 mM Tris pH 8.5, 50 mM $MgCl_2$ and 25 % pentaerythritol propoxylate 629. After 7 days, $100 \times 150 \times 40$ μm^3 crystals were harvested and frozen by immersion in liquid nitrogen.

Data collection, structure determination and refinement. Data up to 3.3 Å was collected from one of the previously described crystals in the ID23-1 beamline at the European Synchrotron Radiation Facility (ESRF, Grenoble, France). The wavelength used was 0.9795 Å, and the detector was Pilatus 6M. A total of 730 diffraction images were taken by oscillating the crystal in steps of 0.1 °. These images were processed using the XDS program (Kabsch, 2010). Empty particle crystal belonged to the space group H3 with unit cell parameters: 305.59 Å, 305.59 Å, 796.49 Å, 90°, 90° and 120°. During the processing, the resolution was cut to 3.6 Å using the CC1/2 criteria as the cut-off (Karplus & Diederichs, 2012). An initial model of the TrV empty particle was obtained by molecular replacement using the program Phaser (McCoy *et al.*, 2007). The protomer of the TrV mature capsid (RCSB PDB code 3NAP; Squires *et al.*, 2013) was used as the search model. Twenty protomers were located in the asymmetric unit of the empty capsid crystal. At this point, the absence of electron density for the N-terminal regions of VP1 and VP2 was evident and therefore, these residues were removed from the initial model. The test set was generated separating 2 % of the reflections in thin-resolution shells. The initial model was refined with Refmac5 (Murshudov *et al.*, 2011) using 20-fold non-crystallographic symmetry constraints. Iterative refinement cycles were combined with density averaging, solvent flattening and histogram matching cycles using density-modification (Cowtan & Main, 1998) and with manual building using Coot (Emsley *et al.*, 2010). Final refinement statistics are shown in Table 1.

Illustrations were produced using PyMOL and Chimera (Pettersen *et al.*, 2004). Interactions between proteins were calculated using the software Protein Interactions Calculator (Tina *et al.*, 2007).

ACKNOWLEDGEMENTS

We thank the local contact at the ESRF for providing technical assistance in using beamline ID23-1.

R. S.-E. was supported by a predoctoral fellowship from the Basque Government (BG). I. L.-M. is recipient of a predoctoral fellowship from the Fundación Biofísica Bizkaia (FBB), Spain. The work of G. A. M. was partially supported by Consejo Nacional de Investigaciones Científicas y Técnicas (CONICET, PIP2011-0007), Comisión de Investigaciones Científicas de la Provincia de Buenos Aires (CICPBA), Agencia Nacional de Promoción Científica y Técnica, Argentina (PICT N_ 2011-1081) and University of La Plata. This work was partially supported by grants from the BG (MV-2012-2-41, AE-2012-1-44, S-PE12FB001), Universidad del País Vasco (UPV/EHU) (IT849-13, OTRI code 2013.0666) and Ministerio de Ciencia e Innovación (MICINN) (BFU2012-36241), Spain.

REFERENCES

Agirre, J., Aloria, K., Arizmendi, J. M., Iloro, I., Elortza, F., Sánchez-Eugenia, R., Marti, G. A., Neumann, E., Rey, F. A. & Guérin, D. M. (2011). Capsid protein identification and analysis of mature Triatoma virus (TrV) virions and naturally occurring empty particles. *Virology* **409**, 91–101.

Agirre, J., Goret, G., LeGoff, M., Sánchez-Eugenia, R., Marti, G. A., Navaza, J., Guérin, D. M. & Neumann, E. (2013). Cryo-electron microscopy reconstructions of triatoma virus particles: a clue to unravel genome delivery and capsid disassembly. *J Gen Virol* **94**, 1058–1068.

Bakker, S. E., Groppelli, E., Pearson, A. R., Stockley, P. G., Rowlands, D. J. & Ranson, N. A. (2014). Limits of structural plasticity in a picornavirus capsid revealed by a massively expanded equine rhinitis a virus particle. *J Virol* **88**, 6093–6099.

Baxt, B. & Bachrach, H. L. (1980). Early interactions of foot-and-mouth disease virus with cultured cells. *Virology* **104**, 42–55.

Belnap, D. M., Filman, D. J., Trus, B. L., Cheng, N., Booy, F. P., Conway, J. F., Curry, S., Hiremath, C. N., Tsang, S. K. & other authors (2000). Molecular tectonic model of virus structural transitions: the putative cell entry states of poliovirus. *J Virol* **74**, 1342–1354.

Bennett, M. J., Schlunegger, M. P. & Eisenberg, D. (1995). 3D domain swapping: a mechanism for oligomer assembly. *Protein Sci* **4**, 2455–2468.

Bonning, B. C. & Miller, W. A. (2010). Dicistroviruses. *Annu Rev Entomol* **55**, 129–150.

Bostina, M., Levy, H., Filman, D. J. & Hogle, J. M. (2011). Poliovirus RNA is released from the capsid near a twofold symmetry axis. *J Virol* **85**, 776–783.

Brown, F. & Cartwright, B. (1961). Dissociation of foot-and-mouth disease virus into its nucleic acid and protein components. *Nature* **192**, 1163–1164.

Bubeck, D., Filman, D. J., Cheng, N., Steven, A. C., Hogle, J. M. & Belnap, D. M. (2005). The structure of the poliovirus 135S cell entry intermediate at 10-angstrom resolution reveals the location of an externalized polypeptide that binds to membranes. *J Virol* **79**, 7745–7755.

Cowtan, K. & Main, P. (1998). Miscellaneous algorithms for density modification. *Acta Crystallogr Sect D Biol Crystallogr* **54**, 487–493.

Czibener, C., La Torre, J. L., Muscio, O. A., Ugalde, R. A. & Scodeller, E. A. (2000). Nucleotide sequence analysis of Triatoma virus shows that it is a member of a novel group of insect RNA viruses. *J Gen Virol* **81**, 1149–1154.

Emsley, P., Lohkamp, B., Scott, W. G. & Cowtan, K. (2010). Features and development of Coot. *Acta Crystallogr Sect D Biol Crystallogr* **66**, 486–501.

Garriga, D., Pickl-Herk, A., Luque, D., Wruss, J., Castón, J. R., Blaas, D. & Verdaguer, N. (2012). Insights into minor group rhinovirus uncoating: the X-ray structure of the HRV2 empty capsid. *PLoS Pathog* **8**, e1002473.

Grant, R. A., Hiremath, C. N., Filman, D. J., Syed, R., Andries, K. & Hogle, J. M. (1994). Structures of poliovirus complexes with anti-viral drugs: implications for viral stability and drug design. *Curr Biol* **4**, 784–797.

Grayson, M., Clayton, J., Coura, J. R., Viñas, P. A. & Petherick, A. (2010). Chagas disease. *Nature* **115**, S3–S22.

Hewat, E. A., Neumann, E. & Blaas, D. (2002). The concerted conformational changes during human rhinovirus 2 uncoating. *Mol Cell* **10**, 317–326.

Hewat, E. A. & Blaas, D. (2004). Cryoelectron microscopy analysis of the structural changes associated with human rhinovirus type 14 uncoating. *J Virol* **78**, 2935–2942.

Kabsch, W. (2010). XDS. *Acta Crystallogr Sect D Biol Crystallogr* **66**, 125–132.

Karplus, P. A. & Diederichs, K. (2012). Linking crystallographic model and data quality. *Science* **336**, 1030–1033.

Levy, H. C., Bostina, M., Filman, D. J. & Hogle, J. M. (2010). Catching a virus in the act of RNA release: a novel poliovirus uncoating intermediate characterized by cryo-electron microscopy. *J Virol* **84**, 4426–4441.

Marti, G. A., Echeverría, M. G., Susevich, M. L., Ceccarelli, S., Balsalobre, A., Rabinovich, G. M. J., Solorzano, E., Monroy, C. & other authors (2013). Exploration for Triatoma virus (TrV) infection in laboratory-reared triatomines of Latin America: a collaborative study*. *Int J Trop Insect Sci* **33**, 294–304.

Mayo, M. A. (2002). Virus taxonomy – Houston 2002. *Arch Virol* **147**, 1071–1076.

McCoy, A. J., Grosse-Kunstleve, R. W., Adams, P. D., Winn, M. D., Storoni, L. C. & Read, R. J. (2007). Phaser crystallographic software. *J Appl Crystallogr* **40**, 658–674.

Murshudov, G. N., Skubák, P., Lebedev, A. A., Pannu, N. S., Steiner, R. A., Nicholls, R. A., Winn, M. D., Long, F. & Vagin, A. A. (2011). REFMAC 5 for the refinement of macromolecular crystal structures. *Acta Crystallogr Sect D Biol Crystallogr* **67**, 355–367.

Muscio, O. A., La Torre, J. L. & Scodeller, E. A. (1988). Characterization of Triatoma virus, a picorna-like virus isolated from the triatomine bug *Triatoma infestans*. *J Gen Virol* **69**, 2929–2934.

Muscio, O. A., La Torre, J., Bonder, M. A. & Scodeller, E. A. (1997). Triatoma virus pathogenicity in laboratory colonies of *Triatoma infestans* (Hemiptera: Reduviidae). *J Med Entomol* **34**, 253–256.

Panjwani, A., Strauss, M., Gold, S., Wenham, H., Jackson, T., Chou, J. J., Rowlands, D. J., Stonehouse, N. J., Hogle, J. M. & Tuthill, T. J. (2014). Capsid protein VP4 of human rhinovirus induces membrane permeability by the formation of a size-selective multimeric pore. *PLoS Pathog* **10**, e1004294.

Pettersen, E. F., Goddard, T. D., Huang, C. C., Couch, G. S., Greenblatt, D. M., Meng, E. C. & Ferrin, T. E. (2004). UCSF Chimera – a visualization system for exploratory research and analysis. *J Comput Chem* **25**, 1605–1612.

Pickl-Herk, A., Luque, D., Vives-Adrián, L., Querol-Audí, J., Garriga, D., Trus, B. L., Verdaguer, N., Blaas, D. & Castón, J. R. (2013). Uncoating of common cold virus is preceded by RNA switching as determined by X-ray and cryo-EM analyses of the subviral a-particle. *Proc Natl Acad Sci U S A* **110**, 20063–20068.

Querido, J. F. B., Agirre, J., Marti, G. A., Guérin, D. M. A. & Silva, M. S. (2013). Molecular techniques for dicistrovirus detection without RNA extraction or purification. *Biomed Res Int* **2013**, 218593.

Ren, J., Wang, X., Hu, Z., Gao, Q., Sun, Y., Li, X., Porta, C., Walter, T. S., Gilbert, R. J. & other authors (2013). Picornavirus uncoating intermediate captured in atomic detail. *Nat Commun* **4**, 1929.

Rossmann, M. G., He, Y. & Kuhn, R. J. (2002). Picornavirus–receptor interactions. *Trends Microbiol* **10**, 324–331.

Shingler, K. L., Yoder, J. L., Carnegie, M. S., Ashley, R. E., Makhov, A. M., Conway, J. F. & Hafenstein, S. (2013). The enterovirus 71 A-particle forms a gateway to allow genome release: a cryoEM study of picornavirus uncoating. *PLoS Pathog* **9**, e1003240.

Smith, T. J., Kremer, M. J., Luo, M., Vriend, G., Arnold, E., Kamer, G., Rossmann, M. G., McKinlay, M. A., Diana, G. D. & Otto, M. J. (1986). The site of attachment in human rhinovirus 14 for antiviral agents that inhibit uncoating. *Science* **233**, 1286–1293.

Smyth, M., Tate, J., Hoey, E., Lyons, C., Martin, S. & Stuart, D. (1995). Implications for viral uncoating from the structure of bovine enterovirus. *Struct Biol* **2**, 224–231.

Snijder, J., Uetrecht, C., Rose, R. J., Sanchez-Eugenia, R., Marti, G. A., Agirre, J., Guérin, D. M., Wuite, G. J., Heck, A. J. & Roos, W. H. (2013). Probing the biophysical interplay between a viral genome and its capsid. *Nat Chem* **5**, 502–509.

Squires, G., Pous, J., Agirre, J., Rozas-Dennis, G. S., Costabel, M. D., Marti, G. A., Navaza, J., Bressanelli, S., Guérin, D. M. & Rey, F. A. (2013). Structure of the Triatoma virus capsid. *Acta Crystallogr D Biol Crystallogr* **69**, 1026–1037.

Sánchez-Eugenia, R., Goikolea, J., Gil-Cartón, D., Sánchez-Magraner, L. & Guérin, D. M. A. (2015a). Triatoma virus recombinant VP4 protein induces membrane permeability through dynamic pores. *J Virol* **89**, 4645–4654.

Sánchez-Eugenia, R., Méndez, F., Querido, J. F. B., Silva, M. S., Guérin, D. M. & Rodríguez, J. F. (2015b). Triatoma virus structural polyprotein expression, processing and assembly into virus-like particles. *J Gen Virol* **96**, 64–73.

Tate, J., Liljas, L., Scotti, P., Christian, P., Lin, T. & Johnson, J. E. (1999). The crystal structure of cricket paralysis virus: the first view of a new virus family. *Nat Struct Biol* **6**, 765–774.

Tina, K. G., Bhadra, R. & Srinivasan, N. (2007). PIC: protein interactions calculator. *Nucleic Acids Res* **35**, W473–W476.

Tuthill, T. J., Harlos, K., Walter, T. S., Knowles, N. J., Groppelli, E., Rowlands, D. J., Stuart, D. I. & Fry, E. E. (2009). Equine rhinitis a virus and its low pH empty particle: clues towards an aphthovirus entry mechanism? *PLoS Pathog* **5**, e1000620.

Wang, X., Peng, W., Ren, J., Hu, Z., Xu, J., Lou, Z., Li, X., Yin, W., Shen, X. & other authors (2012). A sensor-adaptor mechanism for enterovirus uncoating from structures of EV71. *Nat Struct Mol Biol* **19**, 424–429.

Wang, X., Ren, J., Gao, Q., Hu, Z., Sun, Y., Li, X., Rowlands, D. J., Yin, W., Wang, J. & other authors (2015). Hepatitis A virus and the origins of picornaviruses. *Nature* **517**, 85–88.

Xing, L., Casasnovas, J. M. & Cheng, R. H. (2003). Structural analysis of human rhinovirus complexed with ICAM-1 reveals the dynamics of receptor-mediated virus uncoating. *J Virol* **77**, 6101–6107.

Zhang, X., Settembre, E., Xu, C., Dormitzer, P. R., Bellamy, R., Harrison, S. C. & Grigorieff, N. (2008). Near-atomic resolution using electron cryomicroscopy and single-particle reconstruction. *Proc Natl Acad Sci U S A* **105**, 1867–1872.

Zhao, R., Hadfield, A. T., Kremer, M. J. & Rossmann, M. G. (1997). Cations in human rhinoviruses. *Virology* **227**, 13–23.